International Journal of Science and Research Archive

eISSN: 2582-8185

Cross Ref DOI: 10.30574/ijsra

Journal homepage: https://ijsra.net/

(RESEARCH ARTICLE)

Check for updates

Preparation and characterization of chitosan and hydroxyapatite composite

Sreekanta Nath Dalal *, Suman Chandra Roy and Shah Md. Masum

Department of Applied Chemistry and Chemical Engineering, Faculty of Engineering & Technology, University of Dhaka, Bangladesh.

International Journal of Science and Research Archive, 2024, 12(02), 1477–1492

Publication history: Received on 22 June 2024; revised on 28 July 2024; accepted on 31 July 2024

Article DOI: https://doi.org/10.30574/ijsra.2024.12.2.1327

Abstract

Chitosan and hydroxyapatite (HAp) composites were prepared at different ratios (60% chitosan & 40% HAp, 50% chitosan & 50% HAp, 40% chitosan & 60% HAp). The mixtures are dissolved in a 2% acetic acid solution and heated to about 60°C-70°C with continuous stirring for about 1 hour. After that, the solutions are naturally dried on heat-sealing paper placed above a glass sheet. After about 24 hours, chitosan and hydroxyapatite composite films are prepared.

Fourier Transform Infrared Spectroscopy (FTIR) analysis showed that Hydroxyapatite is mainly found at lower wave numbers in the range 400–600 cm^{-1}. X-ray diffraction patterns were showed, the crystalline properties of the composites increase with Hydroxyapatite. Differential Thermal Gravimetry (DTG) analysis of the composites indicated that the material is thermally stable up to 300°C.

This paper aims to review the literature concerning chitosan-hydroxyapatite composites for bone restoration and discuss the primary methods of preparation and mechanical properties of these materials.

Keywords: Chitosan; Hydroxyapatite (HAp); Composite; Polymer; Chitin

1. Introduction

Bone repair or regeneration is a common and complex clinical challenge in orthopedic surgery. Every year, millions of people suffer from bone diseases arising from trauma, tumors, or bone fractures, and unfortunately, some die due to the lack of an ideal bone substitute [1],[2]. Metallic implants are widely used in many treatments and are fairly successful. However, they do not provide optimal therapy due to shortcomings such as stress shielding during post-healing, chronic inflammation caused by corrosion, and fatigue and loosening of the implant. Consequently, a second surgery is often required to remove the metallic implant. Although autogenic bone performs better in terms of biocompatibility and other factors, it also necessitates secondary surgery to procure donor bone from the patient's own body [1].

A desirable material for use in clinical orthopedics is a biodegradable, biomimetic material that induces and promotes new bone formation by osteogenic cells at the required site. Ideally, these materials should be in the form of scaffolds, which provide space for tissue development and offer temporary mechanical support. Potentially suitable biomaterials for use in bone tissue engineering include ceramics (e.g., hydroxyapatite (HAp)) and polymers. In the presented paper, chitosan (Ch) was used as the polymer. Chitosan is a linear polysaccharide composed of β-(1,4)-2-amino-2-deoxy-d-glucopyranose (GlcN) and 2-acetamido-2-deoxy-d-glucopyranose (GlcNAc) residues [3]. It has numerous commercial and potential biomedical uses. Chitosan is a bio-copolymer comprising of glucosamine and *N*-acetylglucosamine, obtained by deacetylation of chitin [4], which is the structural element in the exoskeleton of crustaceans (crabs, shrimp,

* Corresponding author: Sreekanta Nath Dalal

etc.) and cell walls of fungi. The degree of deacetylation (DDA) can be determined by NMR spectroscopy, and the DDA in commercial chitosan ranges from 60% to 100%.

2. Material and methods

2.1. Materials

Shrimp shell waste peeled from the Penaeus monodon species was collected from a food processing landing zone in the southwest part of Khulna division, Bangladesh. The approximate body length of the raw shrimp tail-head was 28 cm (without chelipeds and antennae), and the internal average diameter of the carapace was 4 cm. The shrimp shells were washed thoroughly with distilled water and dried in the sun for 2-3 days. The dried shrimp carapaces were preserved in moisture-proof polyethylene packages.

The shrimp carapaces were used in this investigation for the isolation of chitin and chitosan through demineralization, deproteinization, and deacetylation processes. The chemicals required for the extraction of chitin included HCl (for demineralization), NaOH (for deproteinization and deacetylation), and CH3CH2OH (for decolorization). For dissolution, CH3COOH, KCl, NaCl, CH3COONa, LiCl-DMAc, and HCOOH were required.

Hydroxyapatite (HAp) powder was extracted from the cortical part of long pig bones. Two kinds of HAp were available: after the standard preparation technique, the material was heated to temperatures of 450 °C and 700 °C [5].

Chemical analysis of both samples is comparable and yields the following results:

Powder heated at 450 °C: CaO – 51.91%; P2O5 – 38.25%; MgO – 0.60%; Na2O – 2.84%.

Powder heated at 700 °C: CaO – 52.30%; P2O5 – 38.66%; MgO – 0.59%; Na2O – 2.06%.

2.2. Methods

2.2.1. Extraction method of Chitosan

The extraction of chitosan from shrimp carapace involves a series of chemical treatments. The collected shrimp shells were first washed and dried, then the size was reduced by crushing them manually. The broken carapaces were then ready for chemical treatment. The treatments included demineralization, deproteinization, and decolorization; through these processes, chitin was obtained. The chitin then underwent a chemical treatment called deacetylation to produce chitosan.

2.2.2. Demineralization of Native Shrimp Shells (Carapace)

The shrimp shells were broken into approximately 0.25 cm x 0.5 cm pieces. Demineralization was carried out in a 2M HCl solution bath under constant stirring at ambient temperature. The ratio of shrimp shells to 2M HCl was 1:20. In this process, HCl reacts with mineralized carbonates (mainly CaCO3), forming water-soluble CaCl2 and emitting CO2 gas, as represented in the following reaction:

$$CaCO3+2M\ HCl \rightarrow CaCl2+H2O+CO2\uparrow \text{ (Demineralization)}$$

The endpoint of the demineralization was determined by Armin's method. A solution of 5% ammonium hydroxide and 5% ammonium oxalate was added to 5 ml of the decalcifying medium at intervals. The formation of a cloudy solution caused by the precipitation of calcium oxalate indicated that the specimen was not thoroughly decalcified. The decalcifying solution was replaced repeatedly until the cloudy solution no longer formed. A transparent solution indicated that no more calcium was being removed from the cuticle. The demineralization was completed within 2 hours. After demineralization, the solid product was washed repeatedly with water to reduce the acid content in the solid [6],[7],[8],[3],[9].

2.2.3. Alcohol Treatment of Demineralized Carapace

The demineralized carapace was washed by means of distilled water then a series of alcohol treatment was carried out. The carapace was then treated sequentially with 10%, 30%, 50%, 70% and 90% alcohol solution each carried out for 30 min. After this treatment the carapace was treated with absolute alcohol for 24 hours at room temperature.

2.2.4. Deproteinization of Shrimp Shells for Chitin Extraction

The demineralized chitin-protein complex of the shrimp shells was deproteinized by treatment with 2M NaOH at 55°C for 24 hours with gentle stirring. The ratio of demineralized shell to 2M NaOH was 1:15. The amide bond was hydrolyzed in an alkaline medium to yield a long-chain aliphatic alcohol along with a precipitate of sodium carbonate. The reaction is as follows:

Protein (R-CONH2) + 2M NaOH→R-OH + Na2CO3 + NH3 (Deproteinization)

This treatment was repeated several times until the absence of protein was indicated by the absence of color in the medium at the end of treatment. Filtering and washing with deionized water were carried out until the deproteinized solid was completely neutralized. Then, the chitinous materials were refluxed to eliminate traces of protein and coloring materials [10],[11].

2.2.5. Alcohol Treatment of the Deproteinized Shell

The deproteinized carapace was washed with distilled water, followed by a series of alcohol treatments. The carapace was then treated sequentially with 10%, 30%, 50%, 70%, and 90% alcohol solutions, each for 30 minutes. After these treatments, the carapace was treated with absolute alcohol for 24 hours at room temperature. Finally, pure chitin was dried in an electric oven at 55°C for 24 hours. After deproteinization, the residue known as chitin was about 21.88% by weight of the total weight of the shells. The chitin was then further converted into chitosan through the process of deacetylation.

2.2.6. Extraction of Chitosan by Deacetylation of Chitin

Removal of the acetyl groups (CH3C=O) from chitin by treatment with strong NaOH produces chitosan, which is 2-amino-2-deoxy-β-D-glucose. A sharp nomenclature distinction between chitin and chitosan based on the degree of N-deacetylation has not been defined; however, when the degree of deacetylation (DDA) is greater than 70%, it is considered chitosan. The highest degree of deacetylated chitosan was obtained when the deacetylation process was carried out with 50% NaOH at 100°C for 4 hours (chitin to liquor ratio = 1:20). After this process, solid samples were washed continuously with distilled water and filtered to retain the solid matter, which is chitosan.

The samples were then left uncovered and oven-dried at 55°C for 24 hours. The creamy white chitosan was kept in a moisture-proof packet for further study.

2.2.7. Alcohol Treatment of the Deacetylated Shell

The deacetylated carapace was washed with distilled water, followed by a series of alcohol treatments. The carapace was then treated sequentially with 10%, 30%, 50%, 70%, and 90% alcohol solutions, each for 30 minutes. After these treatments, the carapace was treated with absolute alcohol for 24 hours at room temperature.

2.2.8. Preparation of Chitosan Film

Chitosan film is relatively easy to prepare but difficult to handle due to curving during the drying phase if no assisting means or weights are used to keep it straight. In liquid, it becomes soft and swells, which makes feasible research hard. Chitosan is soluble in mild acids such as acetic acid, lactic acid, citric acid, hydrogen chloride solution, and formic acid. The properties of the films may vary when different acids are used. Acetic acid was used in these experiments.

A measured amount of chitosan prill (extracted from shrimp shell) and distilled water was added into an 80 ml beaker and stirred until the chitosan became wet. Acetic acid was added continuously and mixed until the liquid became homogeneous and clear, which takes around 0.5-1 hour. The desired amount of solution was introduced into the petri dish. The viscosity of the chitosan solution is quite high, like syrup. A measured volume of solution was introduced into the petri dish. The glasses with chitosan solution were placed over a water bath for 24 hours. After this drying phase, the chitosan film was treated with 2M sodium hydroxide (NaOH) liquid for 5 minutes. This helps in the removal of the chitosan film from the petri dish. During the drying phase, the chitosan film also forms onto the edge of the petri dish as well as on the bottom. A surgical knife was used to cut the edge, and the cylindrical shape of the film was maintained. This helps in the removal of the film as an entity from the glass and later in the attachment with Cell-Crown. Then the film was neutralized by bathing it in distilled water.

It was noticed during the experiment that the chitosan film was the easiest to handle when the thickness was between 120-200 μm. Below 100 μm it requires very gentle and careful handling. Also, when the chitosan solution is dried in 6-

and 24-well plates, the final film is easy to attach with Cell-Crown 6 and Cell-Crown 12. With those samples, it was possible to place the ring part of Cell-Crown into the bottom of the well plate, put the film on top of it, and push the body of Cell-Crown on top of the film. It is possible to use the chitosan film immediately for the desired tests or to dry it in a Cell-Crown insert and use it later. Upon drying of the chitosan film, some weight is needed on top of the Cell-Crown or it needs to be pushed down to the bottom of the well plate. When wetted again, the chitosan film becomes soft and swells. Therefore, the Cell-Crown may need to be opened, the film straightened again, and the ring put back in place [12],[8].

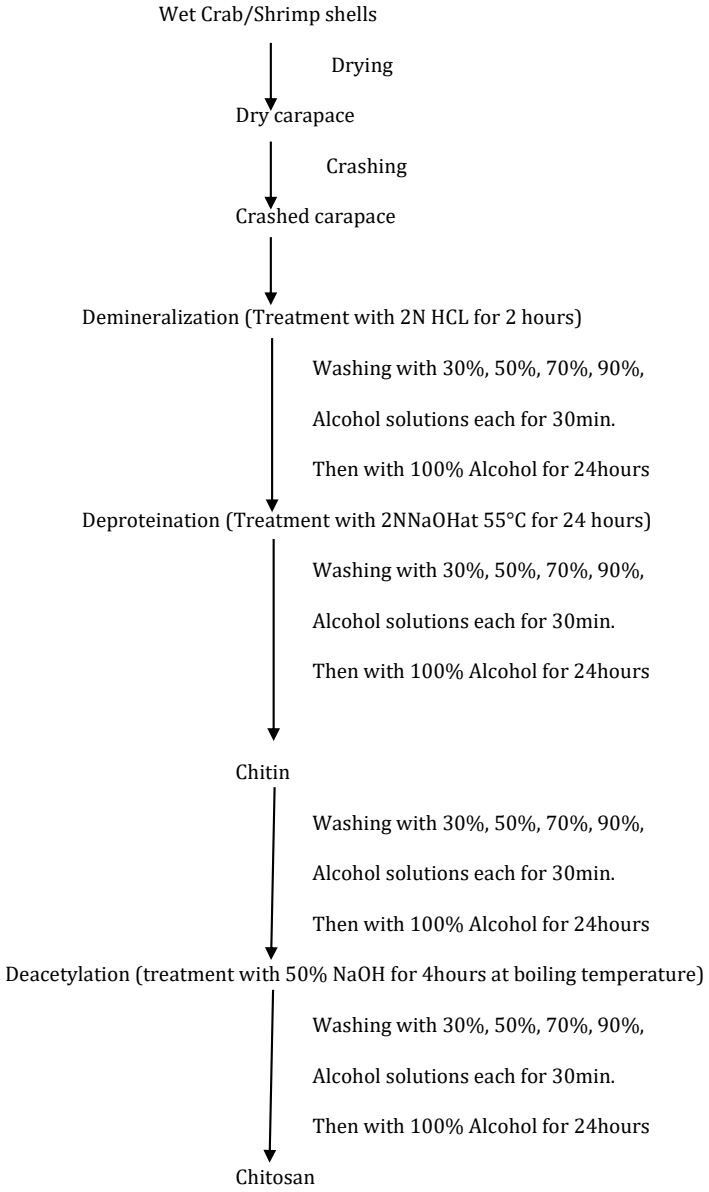

Flow diagram 1 Chitosan production flow diagram

2.2.9. Preparation of Chitosan & Hydroxyapatite Composite

Chitosan and hydroxyapatite are mixed properly at different ratios (60% chitosan & 40% HAp, 50% chitosan & 50% HAp, 40% chitosan & 60% HAp). The mixtures are dissolved in a 2% acetic acid solution (about 1 g sample in 50 ml solution). Then the solutions are heated to about 60°C-70°C with continuous stirring for about 1 hour. After that, the solutions are naturally dried on heat-sealing paper placed above a glass sheet. After about 24 hours, chitosan and hydroxyapatite composite films are prepared [6],[13],[3],[12].

2.3. Characterization of Chitosan and its composites with Hydroxyapatite

2.3.1. Spectroscopic Method

X-ray spectroscopy

X-ray spectroscopy is the most versatile and widely used means of characterizing materials of all forms. There are two general types of structural information that can be studied by X-ray spectroscopy: electronic structure (focused on valence and core electrons, which control the chemical and physical properties, among others) and geometric structure (which gives information about the locations of all or a set of atoms in a molecule at an atomic resolution). This method encompasses several spectroscopic techniques for determining the electronic and geometric structures of the materials using X-ray excitation: X-ray absorption spectroscopy (XAS), X-ray emission spectroscopy (XES), X-ray photoelectron spectroscopy (XPS) and X-ray Auger spectroscopy. Which type of the X-ray spectroscopy is employed depends on whether the target information is electronic, geometric or refers to oxidation states: for instance, XAS (first developed by de Broglie) to probe empty states and the shapes of molecules or local structures, and XPS (first developed by Siegbahn) to investigate occupied electronic states. X-ray spectroscopy is thus a powerful and flexible tool and an excellent complement to many structural analysis techniques such as UV-Vis, IR, NMR or Raman [6],[10],[11].

Fourier Transform Infrared (FTIR) Spectroscopy

Fourier Transform Infrared (FTIR) Spectroscopy is a measurement technique for collecting infrared spectra. Instead of recording the amount of energy absorbed when the frequency of the infra-red light is varied (monochromator), the IR light is guided through an interferometer. After passing through the sample, the measured signal is the interferogram. Performing a mathematical Fourier transform on this signal results in a spectrum identical to that from conventional (dispersive) infrared Spectroscopy [8],[6],[10].

- **Instrumentation**

1. Source: Infrared energy is emitted from a glowing black-body source. This beam passes through an aperture which controls the amount of energy presented to the sample (and, ultimately, to the detector).

2. Interferometer: The beam enters the interferometer where the "spectral encoding" takes place. The resulting interferogram signal then exits the interferometer.

3. Sample: The beam enters the sample compartment where it is transmitted through or reflected off of the surface of the sample, depending on the type of analysis being accomplished. This is where specific frequencies of energy, which are uniquely characteristic of the sample, are absorbed.

4. Detector: The beam finally passes to the detector for final measurement. The detectors used are specially designed to measure the special interferogram.

5. Computer: The measured signal is digitized and sent to the computer where Fourier transformation takes place. The final infrared spectrum is then to the user for interpretation and any further manipulation.

UV-Vis spectroscopy

Ultraviolet/visible (UV-Vis) spectroscopy is useful as an analytical technique for two reasons. Firstly, it can be used to identify certain functional groups in molecules, and secondly, it can be used for assaying. Unlike IR spectroscopy, UV-Vis spectroscopy involves the absorption of electromagnetic radiation from the 200-800 nm range and the subsequent excitation of electrons to higher energy states. The absorption of ultraviolet/visible light by organic molecules is restricted to certain functional groups (chromophores) that contain valence electrons of low excitation energy. The UV-Vis spectrum is complex and appears as a continuous absorption band because the superimposition of rotational and vibrational transitions on the electronic transitions gives a combination of overlapping lines. Nowadays, the individual detection of electron transfers without superimposition by neighboring vibrational bands can also be recorded.

With UV-Vis spectroscopy, it is possible to investigate electron transfers between orbitals or bands of atoms, ions, and molecules existing in the gaseous, liquid, and solid phases. Analysis of solutions and crystals usually takes place in transmission mode, whereas powdered samples are often measured in diffuse reflection mode (Diffuse Reflectance Spectroscopy-DRS). Unlike IR spectroscopy, where Fourier transform techniques predominate, dispersive spectrometers are almost exclusively used in UV-Vis spectroscopy because of the large bandwidths. More details about UV-Vis spectroscopy and its application are presented in many papers and books.

2.3.2. Thermogravimetric Analysis

Thermogravimetric analysis (TGA) of chitosan and chitosan film was conducted using a Thermo-Gravimetric Analyzer (Diamond TGA/DTA) made by Perkin Elmer, which measures the weight loss of a sample as a function of temperature. This is done by placing a sample into a sample holder that hangs from a microgram balance during the entire experiment. The balance mechanism consists of a sample pan holder suspended by a long hang-down wire. The hang-down wire is connected to the balance lever by a small quartz link to prevent static build-up. The weight of the sample holder configuration is electromagnetically balanced on the other side so that the balance can be zeroed before each run. TGA was carried out from room temperature, gradually raised to 600°C at a heating rate of 10°C/min under a nitrogen atmosphere. For high accuracy, every analysis was done two times for each sample.

2.3.3. Tensile Strength Testing

Tensile Strength

Tensile strength measures the force required to pull something, such as a rope, wire, or structural beam, to the point where it breaks.

The breaking load of the cuticle plate was measured in Newton (N).

Stress and strain were calculated using the formula given below.

Tensile Stress (σ) = (Breaking Load)/(Thickness x width)= N/mm^2 = MPa

Tensile Strain (ε) = (Elongation / Initial Length) x 100%

Young's Modulus

Young's modulus, Y, can be calculated by dividing the tensile stress by the tensile strain:

$$Y = FL0/AoΔL$$

Where,

Y is the Young's modulus (modulus of elasticity)

F is the force applied to the object;

Ao is the original cross-sectional area through which the force is applied;

ΔL is the amount by which the length of the object changes;

L0 is the original length of the object.

Percentage of Elongation

The elongation of the test specimen expressed as a percentage of the gage length.

$$\% \text{ of Elongation} = \frac{(\text{Final length} - \text{Original length})}{\text{Original length}} \times 100$$

Specification of Tensile Strength Testing Machine (Hounsfield UTM)

Maximum load 100 N

Speed accuracy - 0.05%

Force accuracy - 0.5%

Types of tests: Tension, Compression Flexure, Shear

Test Materials: Composites

Operation: Fully computerized

Thickness of Films

A digital micrometer was used to measure the film thickness to the nearest 0.001 mm prior to all tests. The film thickness was used for the calculation of tensile strength. For tensile tests, a mean of five measurements across each film specimen was used.

Tensile Test

Tensile measurements for tensile strength, yield strength, elongation, and Young's Modulus were performed using the Instron testing system (model 4411, Instron Engineering Corp., Canton, MA) according to ASTM standard D882. The procedure involved several steps. First, a cardboard holder was prepared using boxboard paper. Then, uniform samples of chitosan film and chitosan derivatives were prepared and inserted in the middle of the holder. After this, the holder containing the sample was attached to the clamp of the Hounsfield machine (fully computer-controlled). The crosshead speed was set at 50 mm/min. The test was then performed, and the data were recorded.

3. Results and discussion

3.1. X-ray spectra of chitosan and composites

Numerous X-ray spectroscopic studies of chitosan and HAp have yielded the diffractive patterns of these compounds. However, different sources have characterized these patterns with differently indexed crystalline peaks. It is also very common to describe the diffraction pattern.

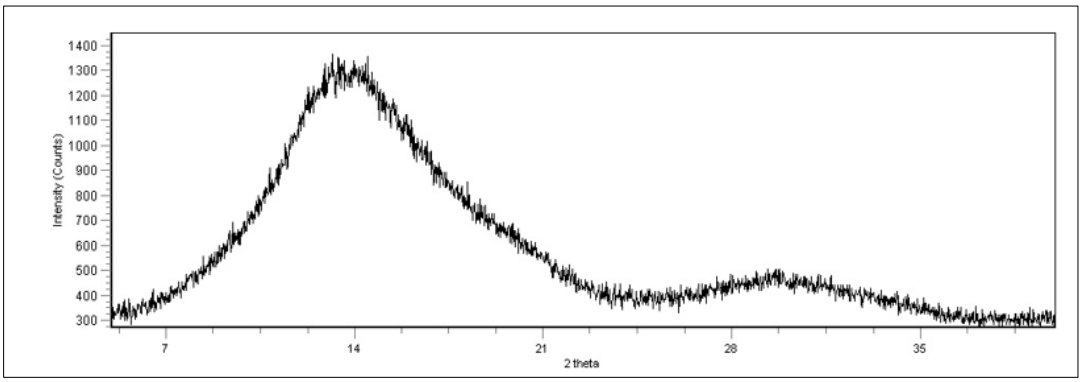

Figure 1 X-ray diffraction spectra of chitosan film

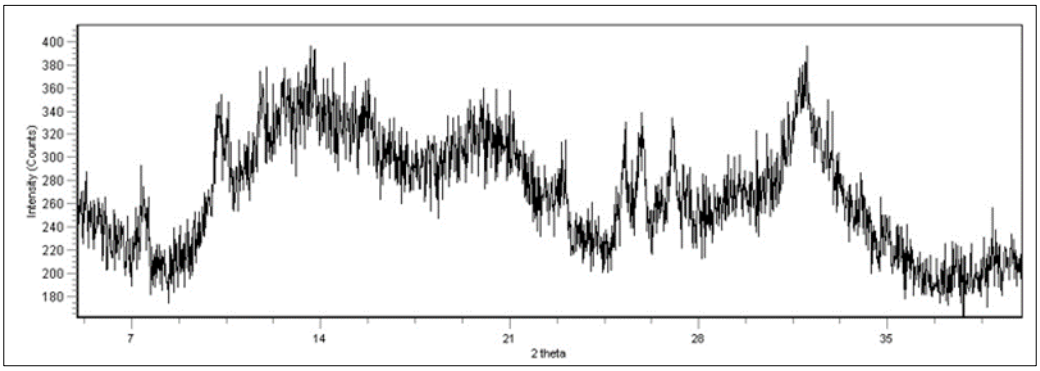

Figure 2 X-ray diffraction spectra of 60% chitosan & 40% HAp

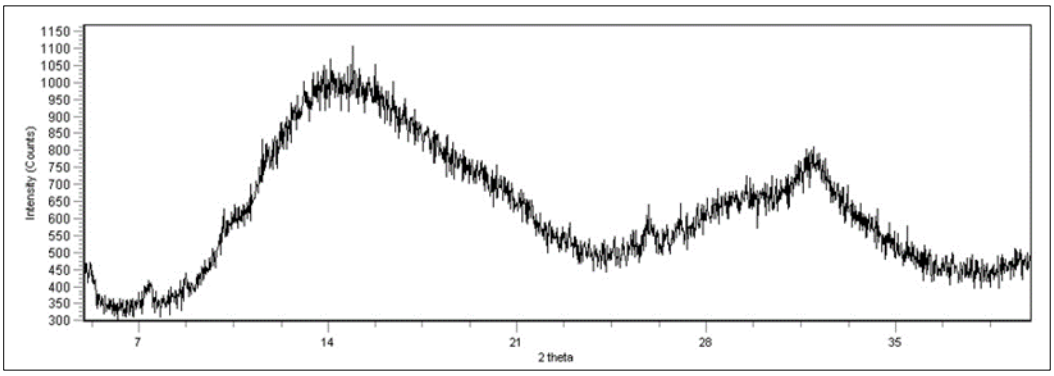

Figure 3 X-ray diffraction spectra of 50% chitosan & 50% HAp

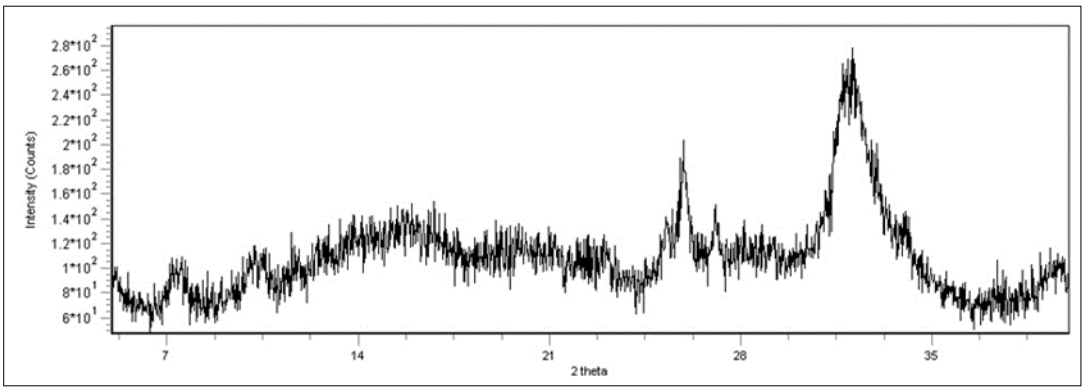

Figure 4 X-ray diffraction spectra of 40% chitosan & 60% HAp

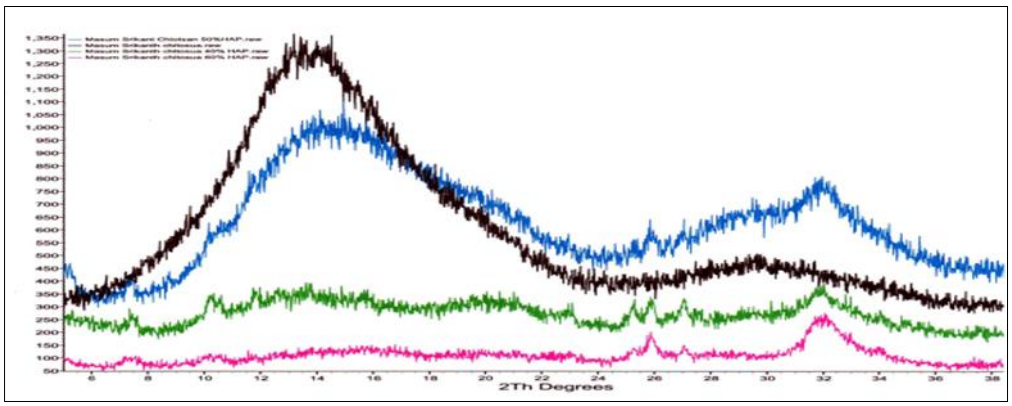

Figure 5 X-ray diffraction spectra of chitosan film (black color), 60% chitosan (green color), 50% chitosan (blue color) & 40% chitosan (red color)

The XRD patterns for the composites suggest that chitosan's amorphous structure decreases and HAp crystallinity increases with increasing content of the HAp. There is a visible broadening of the diffraction peaks with decreasing content of HAp in proportion to chitosan.

3.2. FTIR spectroscopy of chitosan and composites

FTIR spectra are usually recorded in the middle infrared range (4000 cm^{-1} to 400 cm^{-1}) with a resolution of 4 cm^{-1} in the absorbance mode for 8 to 128 scans at room temperature. The samples for FTIR analysis are prepared by grinding the dry blended powders with powdered KBr, often in a ratio of 1:5 (sample: KBr), and then compressed to form discs. Spectra are sometimes measured using a deuterated triglycine sulfate detector (DTGS) with a specific detectivity of 1 x 10^9 cm Hz or on films using the attenuated total reflection (ATR) method in an IR spectrometer. Diffuse Reflectance Infrared Fourier-Transform (DRIFT) spectroscopic analysis is also applied.

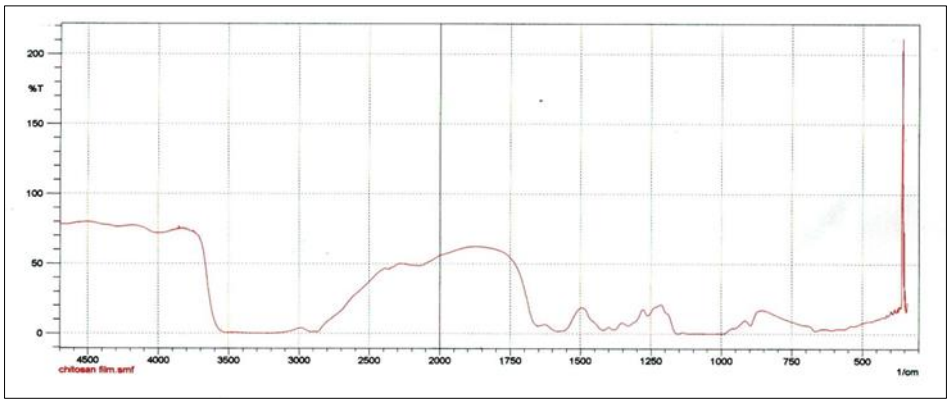

Figure 6 FTIR spectra of chitosan film

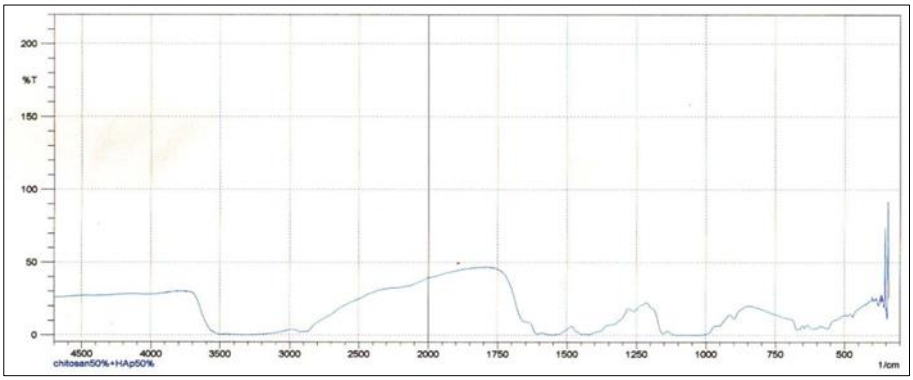

Figure 7 FTIR spectra of 60% chitosan and 40% Hap

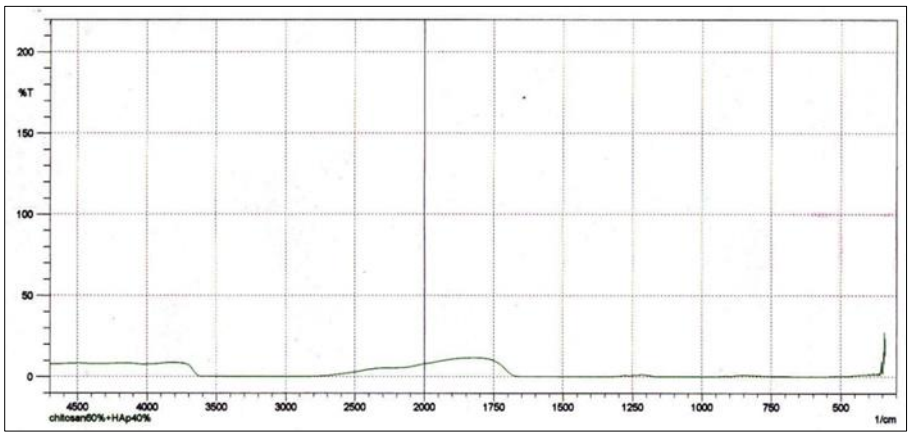

Figure 8 FTIR spectra of 50% chitosan and 50% Hap

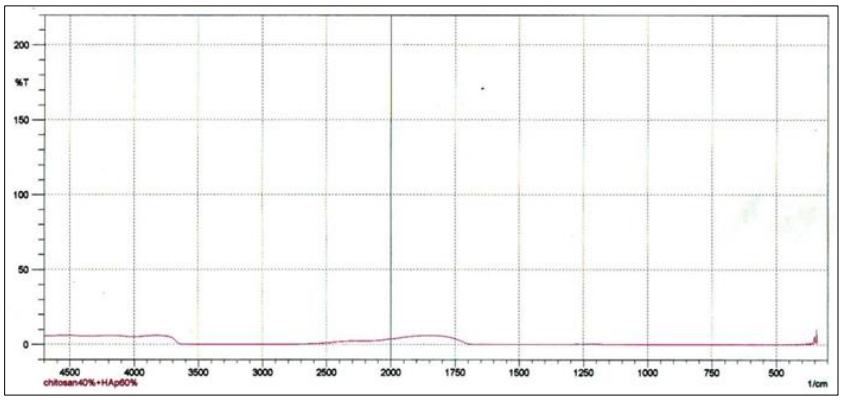

Figure 9 FTIR spectra of 40% chitosan and 60% Hap

The FT-IR spectrum of pure Chitosan shows a characteristic band above 3000 cm^{-1}, which corresponds to stretching vibrations of hydroxyl groups. Also visible are bands representing the =C=O stretching vibrations and the =N–H in-plane bending vibrations characteristic of amide I and II structures, in the wavelength number range from 1650 to 1600 cm^{-1} [6]. Also, a peak characteristic of the amide III structure is visible at 1257 cm^{-1}, whose intensity decreases with increasing HAp content in the composite [6]. The characteristic spectrum of HAp is mainly found at lower wave numbers in the range 400–600 cm^{-1}, which can be associated respectively with stretching and bending vibrations of the PO_4^{3-} group [6].

3.3. UV-Vis spectra of chitosan and composites

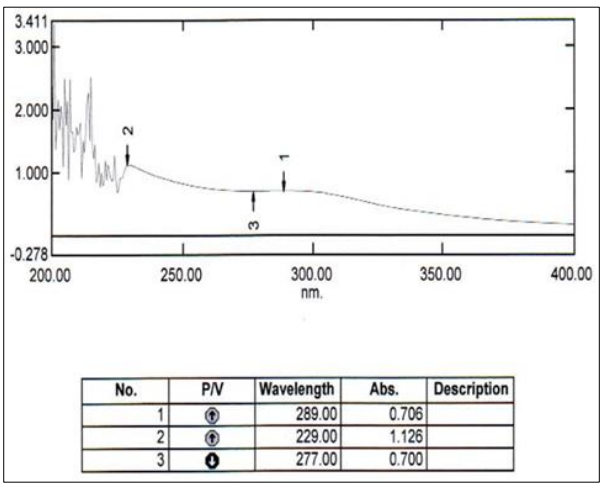

No.	P/V	Wavelength	Abs.	Description
1	↑	289.00	0.706	
2	↑	229.00	1.126	
3	↓	277.00	0.700	

Figure 10 UV spectra of chitosan film

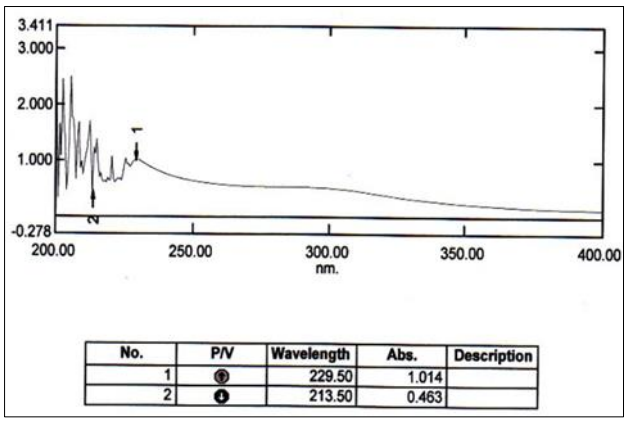

No.	P/V	Wavelength	Abs.	Description
1	↑	229.50	1.014	
2	↓	213.50	0.463	

Figure 11 UV spectra of 60% chitosan and 40% HAp

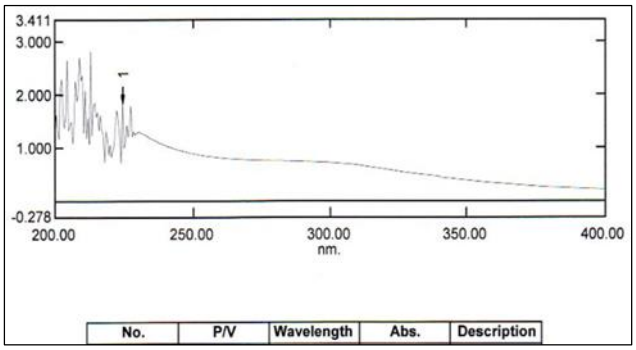

Figure 12 UV spectra of 50% chitosan and 50% Hap

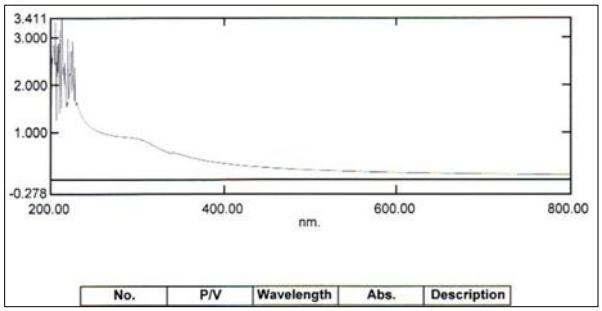

Figure 13 UV spectra of 40% chitosan and 60% HAp

From the UV spectra of the chitosan film, it is shown that it gives absorbance at wavelengths of 229 nm and 289 nm, with maximum absorbance at 229 nm. The peak maximum absorbance pattern indicates that UV absorbance decreases with increasing hydroxyapatite (HAp) content in the composite.

3.4. Thermal Stability (Thermogravimetric Analysis) of chitosan and composites

This analysis was carried out in order to evaluate the thermal stability of the isolated shrimp chitosan film and its composites with hydroxyapatite. DTA, DTG and TGA curves are represented from Figure 14 to Figure 17.

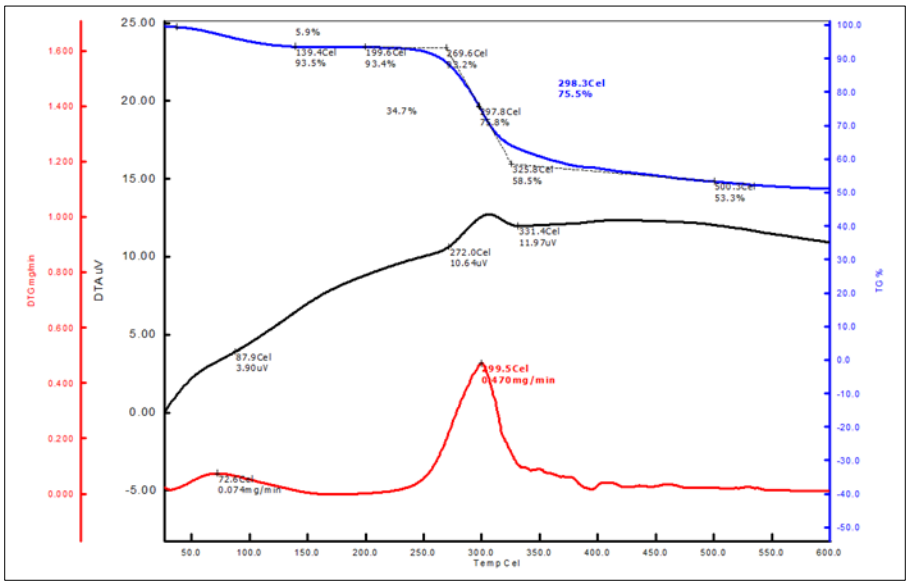

Figure 14 TGA, DTA and DTG curve of chitosan film

TG shows 5.9% initial loss due to moisture. The onset temperature, 75.8% degradation temperature and the maximum slope are at 269.6°C, 297.8°C, 298.3°C. The total degradation is 34.7%. The DTA curve indicates two endothermic peaks at 87.9°C, 331.4°C due to moisture and thermal degradation respectively. The maximum peak is 297.8°C. DTG curve shows two peaks at 72.6°C, 299.5°C. The initial peak is due to elimination of moisture and the second peak is due to one step degradation of chitosan. The maximum peak is 299.5°C.

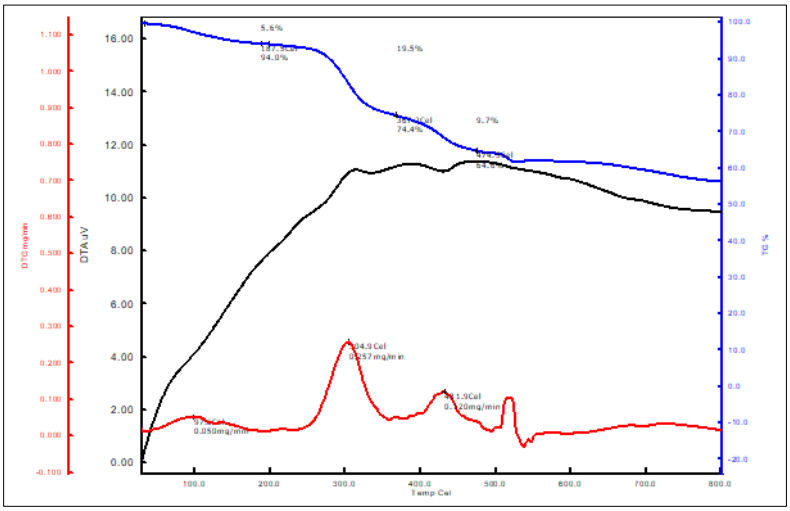

Figure 15 TGA, DTA and DTG curve of 60% chitosan and 40% HAp

TG shows the 5.6% initial loss due to moisture. The onset temperature, 74.4% degradation temperature and the maximum slope are at 187.5°C, 367.2°C. The total degradation is 19.5%. The DTA curve indicates the exothermic peaks at 474.5°C are due to thermal degradation. DTG curve shows three peaks at 97.6 °C, 304.9°C, 431.9°C. The initial peak is due to elimination of moisture and the second peak is due to one step degradation of chitosan. And the third peak is due to degradation of Hydroxyapatite. And the maximum peak is 304.9°C.

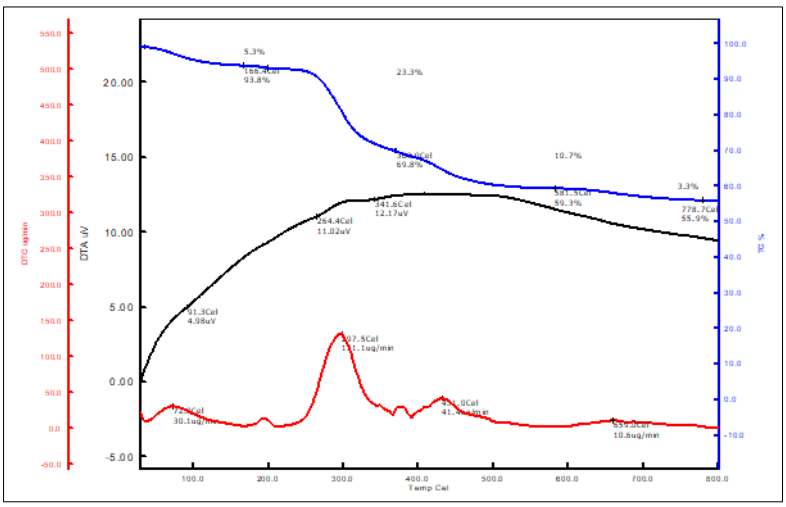

Figure 16 TGA, DTA and DTG curve of 50% chitosan and 50% HAp

The TG curve shows the 5.3% initial weight loss due to moisture. The onset temperature, 69.8% degradation temperature and the maximum slope are at 369.9°C, 581.5°C, 778.7°C. The total degradation is 23.3%. The DTA curve shows one exothermic and one endothermic peak at 91.3°C, 341.6°C are due to moisture and thermal degradation respectively. And the maximum peak is 341.6°C. DTG curve shows three peaks at 72.0°C, 297.5°C, 431.0°C. The initial peak is due to elimination of moisture and the second peak is due to one step degradation of Chitosan and the third peak is due to degradation of Hydroxyapatite. And the maximum peak is 297.5°C.

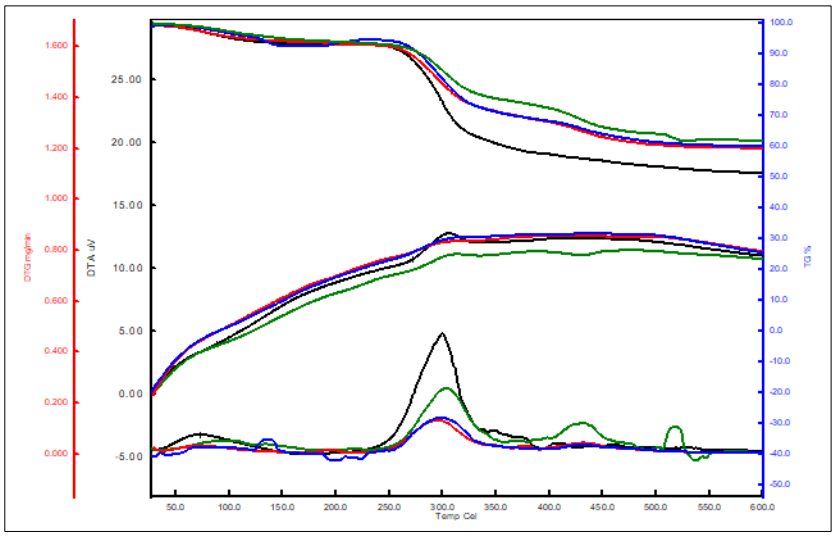

Figure 17 TGA, DTA and DTG curve of chitosan film, 60% chitosan and 40% Hap, 50% chitosan and 50% Hap and 40% chitosan and 60% HAp

From the TG curve, it is observed that thermal degradation decreases with the increasing HAp content in the composite. Additionally, the DTG curve shows that the degradation temperature of chitosan and its composite with HAp is approximately 300°C.

3.5. Tensile Strength of Chitosan Film and Composite

Table 1 Tensile Properties of Chitosan Film

Experiment No.	Tensile Strength, Mpa	Avg. Tensile Strength, Mpa	E Modulus, Mpa	Avg. E-Modulus	% of Elongation	Avg. of % Elongation
1	55.9	51.77	1516	1567	7.98	7.24
2	37.33		885		8.66	
3	33.23		1254		5.1	
4	80.6		2616		7.23	

Table 2 Tensile Properties of 60% Chitosan + 40%HAp

Experiment No.	Tensile Strength, Mpa	Avg. Tensile Strength, Mpa	E Modulus, Mpa	Avg. E-Modulus	% of Elongation	Avg. of % Elongation
1	11.96	13.99	812	852	2.437	2.74
2	13.84		738		2.843	
3	13.84		708		3.187	
4	16.32		1150		2.483	

Table 3 Tensile Properties of 50% Chitosan + 50%HAp

Experiment No.	Tensile Strength, Mpa	Avg. Tensile Strength, Mpa	E Modulus, Mpa	Avg. E-Modulus	% of Elongation	Avg. of % Elongation
1	1.444	8.15	110.7	647	5.08	3.65
2	15.53		1205		3.467	
3	5.89		278		3.15	
4	9.75		996		2.9	

Table 4 Tensile Properties of 40% Chitosan + 60%HAp

Experiment No.	Tensile Strength, Mpa	Avg. Tensile Strength, Mpa	E Modulus, Mpa	Avg. E-Modulus	% of Elongation	Avg. of % Elongation
1	3.287	7.93	460	937	1.496	2.15
2	14.25		1304		1.998	
3	3.452		563		1.756	
4	10.73		1421		3.367	

Table 5 Comparative tensile properties of chitosan film and Composite with HAp

Sample	Tensile Strength (MPa)	E. Modulus (MPa)	% of Elongation
Chitosan	51.77	1567	7.24
Chitosan 50%+Hap 50%	8.15	647	3.65
Chitosan 40%+Hap 60%	7.93	937	2.15
Chitosan 60%+Hap 40%	13.99	852	2.74

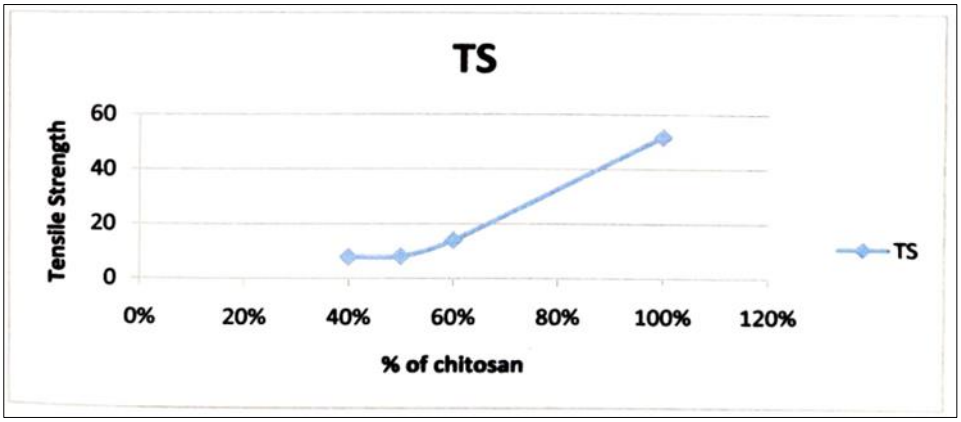

Figure 18 Tensile strength of different composition of Chitosan

From the above study, it can be concluded that chitosan exhibits higher tensile properties. The addition of hydroxyapatite (HAp) decreases the tensile properties as the HAp content increases. However, the chitosan film demonstrates greater flexibility and elongation properties compared to the others. These flexibilities and elongation properties of chitosan film makes it a material, to be applicable in packaging purpose.

4. Conclusion

Chitosan is one of the components most frequently used to prepare calcium phosphate composites, because of its biocompatibility, biodegradation and innocuousness. Due to the interest on composites based on this biopolymer, here we review the state of the art and current trends using Chitosan-based calcium phosphate composites, and especially Hydroxyapatite. Human bone is a hydroxyapatite (HAp) and collagen-based composite.

In this work we try to present some mechanical properties of chitosan & hydroxyapatite such as X-ray diffraction (XRD), FTIR analysis, UV spectrophotometry, TG/DTA analysis, tensile strength, E. modulus, and % elongation.

The study was involved to prepare composites containing chitosan and HAp by natural drying process after proper mixing of chitosan and HAp in 2% acetic acid at about 60°C and also the effect of percentage of chitosan and HAp on the composites. The composites are used to replacement of bone. From this study the following can be conclude that-

- The XRD patterns for the composites suggest that chitosan's amorphous structure decreases and HAp crystallinity increases with increasing content of the HAp.
- FTIR data show that the characteristic spectrum of HAp is mainly found at lower wave numbers in the range 400–600 cm^{-1}, which can be associated respectively with stretching and bending vibrations of the PO_4^{3-} group.
- UV-Visible identification shows nearly about at 229 nm give maximum absorbance and with increasing of HAp composite behaves UV inactive material.
- TG data show that thermal degradation decreases with the increasing HAp content in the composite.
- DTG curve show that the degradation temperature of chitosan and it composite with HAp nearly 300°C.
- The tensile strength of the composite is reduced with increasing HAp.

There are some other method development techniques like chromatography may apply for further study [14].

In Bangladesh there is a bright future of chitosan and chitosan derived products because there is an easy availability of the raw materials as shrimp carapace which is thrown away as waste from sea food processing plant. If this wastage is utilized in chitosan production it can be fruitful for our country.

Compliance with ethical standards

Acknowledgments

The authors are grateful to the University of Dhaka, Bangladesh for financial support. We are thankful to the Bangladesh Council of Scientific and Industrial Research (BCSIR), Dhaka, Bangladesh, for providing analytical support to carry out this research. The research proposal and plan were initiated by Sreekanta Nath Dalal and the amount of publication fees were provided by Sreekanta Nath Dalal.

Disclosure of conflict of interest

The authors disclose no conflicts of interest regarding the publication of this paper.

References

[1] R. Murugan and S. Ramakrishna, "Bioresorbable composite bone paste using polysaccharide based nano hydroxyapatite," *Biomaterials*, vol. 25, no. 17, pp. 3829–3835, Aug. 2004, doi: 10.1016/j.biomaterials.2003.10.016.

[2] J. Venkatesan and S.-K. Kim, "Chitosan Composites for Bone Tissue Engineering—An Overview," *Mar. Drugs*, vol. 8, no. 8, pp. 2252–2266, Aug. 2010, doi: 10.3390/md8082252.

[3] G. Ma, D. Yang, J. F. Kennedy, and J. Nie, "Synthesize and characterization of organic-soluble acylated chitosan," *Carbohydr. Polym.*, vol. 75, no. 3, pp. 390–394, Feb. 2009, doi: 10.1016/j.carbpol.2008.07.035.

[4] F. Zhao *et al.*, "Preparation and histological evaluation of biomimetic three-dimensional hydroxyapatite/chitosan-gelatin network composite scaffolds," *Biomaterials*, vol. 23, no. 15, pp. 3227–3234, Aug. 2002, doi: 10.1016/S0142-9612(02)00077-7.

[5] O. G. Agbabiaka *et al.*, "Effect of calcination temperature on hydroxyapatite developed from waste poultry eggshell," *Sci. Afr.*, vol. 8, p. e00452, Jul. 2020, doi: 10.1016/j.sciaf.2020.e00452.

[6] T. Szatkowski *et al.*, "Synthesis and characterization of hydroxyapatite/chitosan composites," *Physicochem. Probl. Miner. Process. ISSN 2083-3989*, 2015, doi: 10.5277/PPMP150217.

[7] K. S. Katti, D. R. Katti, and R. Dash, "Synthesis and characterization of a novel chitosan/montmorillonite/hydroxyapatite nanocomposite for bone tissue engineering," *Biomed. Mater.*, vol. 3, no. 3, p. 034122, Sep. 2008, doi: 10.1088/1748-6041/3/3/034122.

[8] H.-L. Kim *et al.*, "Preparation and characterization of nano-sized hydroxyapatite/alginate/chitosan composite scaffolds for bone tissue engineering," *Mater. Sci. Eng. C*, vol. 54, pp. 20–25, Sep. 2015, doi: 10.1016/j.msec.2015.04.033.

[9] Q. Hu, "Preparation and characterization of biodegradable chitosan/hydroxyapatite nanocomposite rods via in situ hybridization: a potential material as internal fixation of bone fracture," *Biomaterials*, vol. 25, no. 5, pp. 779–785, Feb. 2004, doi: 10.1016/S0142-9612(03)00582-9.

[10] N. G. Kandile, H. T. Zaky, M. I. Mohamed, A. S. Nasr, and Y. G. Ali, "Extraction and Characterization of Chitosan from Shrimp Shells," *Open J. Org. Polym. Mater.*, vol. 08, no. 03, pp. 33–42, 2018, doi: 10.4236/ojopm.2018.83003.

[11] C. J. Chern and E. Beutler, "Biochemical and electrophoretic studies of erythrocyte pyridoxine kinase in white and black Americans," *Am. J. Hum. Genet.*, vol. 28, no. 1, pp. 9–17, Jan. 1976.

[12] W. Chang, F. Liu, H. R. Sharif, Z. Huang, H. D. Goff, and F. Zhong, "Preparation of chitosan films by neutralization for improving their preservation effects on chilled meat," *Food Hydrocoll.*, vol. 90, pp. 50–61, May 2019, doi: 10.1016/j.foodhyd.2018.09.026.

[13] M. R. Nikpour, S. M. Rabiee, and M. Jahanshahi, "Synthesis and characterization of hydroxyapatite/chitosan nanocomposite materials for medical engineering applications," *Compos. Part B Eng.*, vol. 43, no. 4, pp. 1881–1886, Jun. 2012, doi: 10.1016/j.compositesb.2012.01.056.

[14] Md. N. S. Chowdhury *et al.*, "Robustness Study and Superior Method Development and Validation for Analytical Assay Method of Atropine Sulfate in Pharmaceutical Ophthalmic Solution," *Am. J. Anal. Chem.*, vol. 15, no. 05, pp. 151–164, 2024, doi: 10.4236/ajac.2024.155010.